BOLETÍN GEOLÓGICO Y MINERO 136 (1)
enero-marzo 2025, 009
ISSN-L: 0366-0176, eISSN: 2253-6167
https://doi.org/10.21701/bolgeomin/136.1/009

Boletín Geológico y Minero

RESEARCH ARTICLE

Preliminary Ar-Ar geochronology of Mesozoic alkaline-carbonatitic to tholeiitic magmatism in the Quilengues area, SW Angola

Geocronología Ar-Ar preliminar del magmatismo Mesozoico alcalino-carbonatítico a toleítico del área de Quilengues, SO de Angola

Enrique Merino-Martínez[1*], Pablo Valverde-Vaquero[1], Aratz Beranoaguirre[2,3], Gustavo Galán[2†], Janet Gabites[4], José Manuel[5]

[1]Departamento de Geología y Subsuelo, Centro Nacional Instituto Geológico y Minero de España (IGME-CSIC), 28003 Madrid, España. e.merino@igme.es; p.valverde@igme.es
[2]UTE-PLANAGEO (IGME/LNEG/Impulso), Parque tecnológico de Asturias, parcela 13 A, 33428, Asturias (Spain). Gustavo Galán† Deceased on 2 January 2022
[3]Department of Geosciences, Goethe-University Frankfurt, Altenhöferallee 1, 60438 Frankfurt (Germany). beranoaguirre@em.uni-frankfurt.de
[4]Pacific Center for Isotopic and Geochemical Research, The University of British Columbia, V6T 1Z4, Vancouver, Canada. Janet Gabites, retired
[5]Instituto Geologico de Angola (IGEO), Centralidade do Kilamba, Rua Nr, Luanda (Angola). jose.manuel@igeo.gov.ao

Corresponding author: e.merino@igme.es (Enrique Merino Martínez)

Key point:

New Ar-Ar dating of Cretaceous alkaline-carbonatite and bimodal pulses from SW Angola reveals distinct intrusion episodes.

Lithospheric destabilisation processes induced by the upwelling of alkaline-carbonatite melts during the early stages of the Atlantic rift.

Spatio-temporal migration of alkaline-carbonatite and bimodal pulses associated with the progress of rifting and continental drifting.

ABSTRACT

New geochronological data have been obtained on kimberlitic units related to the Bonga carbonatite massif and basaltic dikes in the Quilengues region of southwestern Angola as part of the National Geological Plan of Angola (PLANAGEO). Ar-Ar dating of mineral separates (phlogopite, amphibole) indicates distinct intrusion pulses for the alkaline-carbonatite magmas of the Bonga Complex (155.2 ± 2.9 Ma) and a NNE-SSW dike assemblage (124.7 ± 2.2 Ma). These ages agree with those reported from coeval volcanic materials in the coastal region, suggesting a direct correlation with lithospheric destabilisation processes induced by the ascent of deep melts, during incipient to progressive stages of the Atlantic rifting and Pangea's breakup. The basaltic dikes may represent the feeding channels of mantle-derived melts that extruded as Large Igneous Provinces (LIPs), forming the Paraná-Angola-Etendeka Province. The spatio-temporal relationships of the studied bodies are consistent with the intrusion of mantle melts during the early stages of rifting, in directions equivalent to the Lucapa structure and the Atlantic margin. The new age data reinforce the existing dataset of Jurassic-Cretaceous alkaline-carbonatite and bimodal (alkaline to tholeiitic) pulses in Angola and their South American counterparts. A structural control is also suggested, with the later alkaline pulses emplaced along ~E-W directions, related to the progress of rifting and the action of deep transform faults during continental breakup.

Keywords: Ar-Ar geochronology; Alkaline-carbonatitic magmas; Bimodal magmatism; Mesozoic; Angola.

Article History:
Received: 02/04/2024
Accepted: 05/03/2025
Published: 22/08/2025

Puntos clave:

Nuevas dataciones Ar-Ar en pulsos cretácicos alcalino-carbonatíticos y bimodales del SO de Angola revelan distintos episodios de intrusión.

Procesos de desestabilización litosférica inducidos por ascenso de fundidos

RESUMEN

Nuevos datos geocronológicos han sido obtenidos en unidades kimberlíticas relacionadas con el macizo carbonatítico de Bonga y en diques basálticos de la región de Quilengues, en el suroeste de Angola, en el marco del Plan Nacional de Geología de Angola (PLANAGEO). Las dataciones Ar-Ar en separados minerales (flogopita, anfíbol) indican distintos pulsos de intrusión para los magmas alcalino-carbonatíticos del Complejo de Bonga (155,2 ± 2,9 Ma) y el conjunto de diques en dirección NNE-SSO (124,7 ± 2,2 Ma). Estas edades concuerdan con aquellas reportadas en materiales volcánicos de la franja litoral, sugiriendo una relación directa con procesos de desestabilización litosférica inducido por el ascenso de fundidos profundos en etapas incipientes a progresivas del *rifting* Atlántico y la ruptura de Pangea. Los diques basálticos, por tanto, podrían representar canales de alimentación de fundidos mantélicos que

alcalino-carbonatíticos en etapas iniciales del *rift* Atlántico.

Migración espacio-temporal de pulsos alcalino-carbonatíticos y bimodales asociados al progreso del *rifting* y la deriva continental.

extruyeron en forma de Grandes Provincias Ígneas (*LIPs*), los cuales conforman la Provincia de Paraná-Angola-Etendeka. Las relaciones espacio-temporales de los cuerpos estudiados están de acuerdo con la intrusión de fundidos mantélicos asociados a estadios incipientes del *rifting*, en direcciones equivalentes a la estructura de Lucapa y del margen Atlántico. Las nuevas edades refuerzan el conjunto de datos existentes sobre la edad de los pulsos alcalinos-carbonatíticos y bimodales (alcalinos a toleíticos) del Jurásico-Cretácico en Angola y en regiones equivalentes de Sudamérica. También se sugiere un control estructural, con el emplazamiento de los pulsos alcalinos más tardíos en direcciones ~E-O, en relación al progreso del *rifting* y a la acción de fallas transformantes profundas durante la ruptura continental.

Palabras clave: Geocronología Ar-Ar; Magmas alcalino-carbonatíticos; Magmatismo bimodal; Mesozoico; Angola.

Historial del artículo:
Recibido: 02/04/2024
Aceptado: 05/03/2025
Publicado: 22/08/2025

Citation / Cómo citar este artículo: Merino-Martínez, E., Valverde-Vaquero, P., Beranoaguirre, A., Galán, G., Gabites, J., Manuel, J. (2025). Preliminary Ar-Ar geochronology of Cretaceous alkaline-carbonatitic to tholeiitic magmatism in the Quilengues area, SW Angola. Boletín Geológico y Minero, 136(1), 009. https://doi.org/10.21701/bolgeomin/136.1/009

1. Introduction

During Mesozoic times, the intrusion of a large diversity of magmas with alkaline and bimodal affinity characterised the central-western part of Angola. These magmas are part of the tectono-thermal events that lead to the destabilisation of Pangaea, and the crustal breakup that promoted the opening of the South Atlantic Ocean (e.g., Coltorti *et al*., 1993; Ernst & Bell, 2010). In this anorogenic cycle, different periods of magmatism occurred with the generation of various plutonic to volcanic bodies of tholeiitic, alkaline, carbonatitic and kimberlitic composition; which were distributed along tectonic alignments that were active during at least the Upper Jurassic and Lower Cretaceous (Cahen *et al*., 1984; Allsopp & Hargraves, 1985; Alberti *et al*., 1999; Comin-Chiaramonti *et al*., 2005, 2007). This magmatism forms part of the same tectonic alignment that has been active since the beginning of the Mesozoic, forming the igneous province of Paraná-Angola-Etendeka (PAE; Issa Filho *et al*., 1991; Alberti *et al*., 1999) or Paraná-Angola-Namibia (PAN; Comin-Chiaramonti *et al*., 2007). A continuous distribution of Mesozoic igneous materials and structural lineaments can be matched across the opposite Angolan and Brazilian continental margins of the South Atlantic Ocean.

While many studies have examined the geochemical features of alkaline to carbonatitic complexes and tholeiitic magmas in southern Angola, few have addressed precise geochronological dating to constrain the timing of magma emplacement. The PAE igneous province of SW Angola was previously dated by the works of Torquato & Amaral (1973), Renne *et al*. (1992, 1996) and Marzoli *et al*. (1999), which reported whole-rock and mineral separate K-Ar and Ar-Ar ages ranging from 222 to 84 Ma for alkaline to tholeiitic basalts in the Kwanza and Namibe basins of Angola's coastal region. But, the alkaline to carbonatitic igneous bodies of southern Angola have not been extensively dated. Silva *et al*. (1973) and Torquato & Amaral (1973) reported whole-rock K-Ar ages between 92 and 82 Ma for some alkaline igneous bodies (syenites, tinguaites and phonolites) from the western portion of Angola, whereas Vale *et al*. (1972) and Allsopp & Hargraves (1985) obtained Rb-Sr and K-Ar ages between 131 and 104 Ma for some nepheline syenite bodies from central-western Angola.

In recent years, the National Geological Plan of Angola (PLANAGEO) has focused on improving the geological knowledge of the country. The UTE PLANAGEO consortium, formed by the *Instituto Geológico y Minero de España* (IGME), the *Laboratório Nacional de Geologia e Energia* of Portugal (LNEG) and the enterprise *Impulso Industrial Alternativo* (IIA) was in charge of the geological, geophysical and geochemical surveys in the southern region of Angola. Within the framework of the PLANAGEO project, a large set of absolute isotopic dating results were obtained on the southern region of Angola. In the most recent igneous materials, presumably of Meso- to Cenozoic age, $^{40}Ar/^{39}Ar$ isotope analyses were conducted on whole-rock and/or on representative mineral separates (e.g., phlogopite, hornblende, plagioclase) in order to constrain their crystallisation age.

This work presents new Ar-Ar geochronological results obtained on selected alkaline and tholeiitic rocks from the Quilengues area of SW Angola. The analysed samples consist of a kimberlitic lava flow related to the carbonatitic magmatism of the Bonga massif, and a basaltic dike that is part of a large alkaline to tholeiitic dike swarm found in the vicinity of the Bonga Complex. $^{40}Ar/^{39}Ar$ stepped heating geochronology is one of the most important techniques for constraining the age of emplacement of these ultrabasic to basic materials (e..g., Renne *et al*., 1996, 1998). The aim of this study is to provide an accurate Ar-Ar dating to better constrain the crystallisation age of these magmas and asses their relation with the various stages of Mesozoic magmatism recorded in southwest Angola, associated with the opening of the South Atlantic Ocean.

2. Geological Setting

The occurrences of Mesozoic alkaline-carbonatitic magmatic rocks in SW Angola are distributed across tectonic lineaments that were active since at least the Upper Jurassic (e.g., Alberti *et al*., 1999), forming what is known as the Lucapa Structure (Lapido-Loureiro, 1968, 1973; Fig. 1A), the Alkaline-carbonatitic Diagonal Trans-Angola Province (Lapido-Loureiro, 1995; Woolley, 2001), the Moçâmedes Arc (Alberti *et al*., 1999), the Khumib region (Comin-Chiaramonti *et al*., 1999, 2005, 2007) or the Volcanic Belt of Angola (Machado, 1959). This magmatism is related to the Mesozoic alkaline to tholeiitic volcanism found along the Angolan coast between Sumbe and Benguela and in the Namibe region of Angola; which forms the Paraná-Angola-Etendeka igneous province, as well as set of dikes, inland, striking almost parallel to the coast (Alberti *et al*., 1992; Peate *et al*., 1992; Marzoli *et al*., 1999; Marsh & Swart, 2018).

The lithology, petrography, mineralogy and structure of the alkaline-carbonatite complexes in Angola are widely described in the works of Lapido-Loureiro (1973), Issa Filho *et al*. (1991), Alberti *et al*. (1999) and Bambi (2015). These works cite the presence of at least 35 alkaline and alkaline-carbonatite complexes in the Republic of Angola. Most complexes form ring structures of highly heterogeneous lithological and mineral composition, showing an evolutionary sequence between the different alkaline and carbonatitic pulses. In SW Angola, these massifs correspond to the Serra da Neve complex and its satellite bodies; Tchivira and Bonga, Chamaco, Belavista, Nonga-Balombo, Chanja, Monte Verde, Elonga, Coola, Longonjo, Chianga, Bailundo, Canata, Chiueca, Capuia and Bangombari.

In the Quilengues area, the alkaline-carbonatite complexes are represented by the Tchivira and Bonga massifs, located approximately 27 km to the south-east of the town of Quilengues (Fig. 1B). These complexes are intrusive in the Palaeoproterozoic (Eburnean) plutono-metamorphic basement, forming inselbergs that reach the highest elevations in the region (2385 m in Tchivira and 1839 m in Bonga; Bambi, 2015; Merino-Martínez & Goicoechea, 2021). This basement is composed of eburnean granites, and leucogranites and scarce mafic bodies overprinted by penetrative and gneissic deformation fabrics, with metamorphism locally reaching migmatisation and partial melting conditions, conforming the so-called Gneiss-Migmatite and Granite Complex (Carvalho, 1982, 1983). This basement has reported whole-rock Rb-Sr ages from 1982 to 1972 Ma for some granitic bodies (Mendes, 1968; Torquato, 1977); and Rb-Sr and K-Ar ages between 1766 and 1643 Ma on mineral separates (muscovite, biotite and/or hornblende) from granites, pegmatites and ultramafic rocks (Mendes, 1968; Silva *et al*., 1973; Torquato, 1977). Other K-Ar ages ranging from 1281 to 644 Ma (Silva *et al*., 1973) have been reported for diverse Mesoproterozoic basic dikes that are intrusive into the Palaeoproterozoic basement in NNW-SSE and WNW-ESE directions.

In the Tchivira massif (Fig. 1B), there is an evolutionary sequence between distinct alkaline and carbonatitic pulses, consisting of an initial intrusion of ring bodies with a strongly alkaline composition (nepheline syenites), followed by various intrusions of ultra-alkaline (nephelinites, ijolites, urtites) and moderately alkaline (alkaline syenites and gabbros) magmas, and a final stage dominated by the intrusion of carbonatitic rocks (Vale *et al*., 1972; Bambi, 2015; Merino-Martínez, 2022). K-Ar and Rb-Sr ages between 138 and 112 Ma have been reported for nepheline syenites from the Tchivira Complex (Vale *et al*., 1972; Allsopp & Hargraves, 1985). The Bonga massif (Fig. 1B) shows a carbonatitic core surrounded by a subvolcanic complex (carbonatites, carbonatitic breccias, syenites, phonolites, trachytes, rhyolites ± lamprophyres). Discrete kimberlitic materials are found in the NW part of the massif embedded in carbonatitic breccias. These polygenetic alkaline-carbonatitic rocks are affected by diverse metasomatic processes and by a complex NW-SE to WNW-ESE and NNE-SSW to NE-SW fracture system (Coltorti *et al*., 1993; Comin-Chiaramonti *et al*., 2007; Melgarejo *et al*., 2012; Bambi, 2015). Bambi (2015) suggests a vertical displacement of approximately 1 km, which uplifted the Bonga subvolcanic massif in relation to the Tchivira plutonic massif.

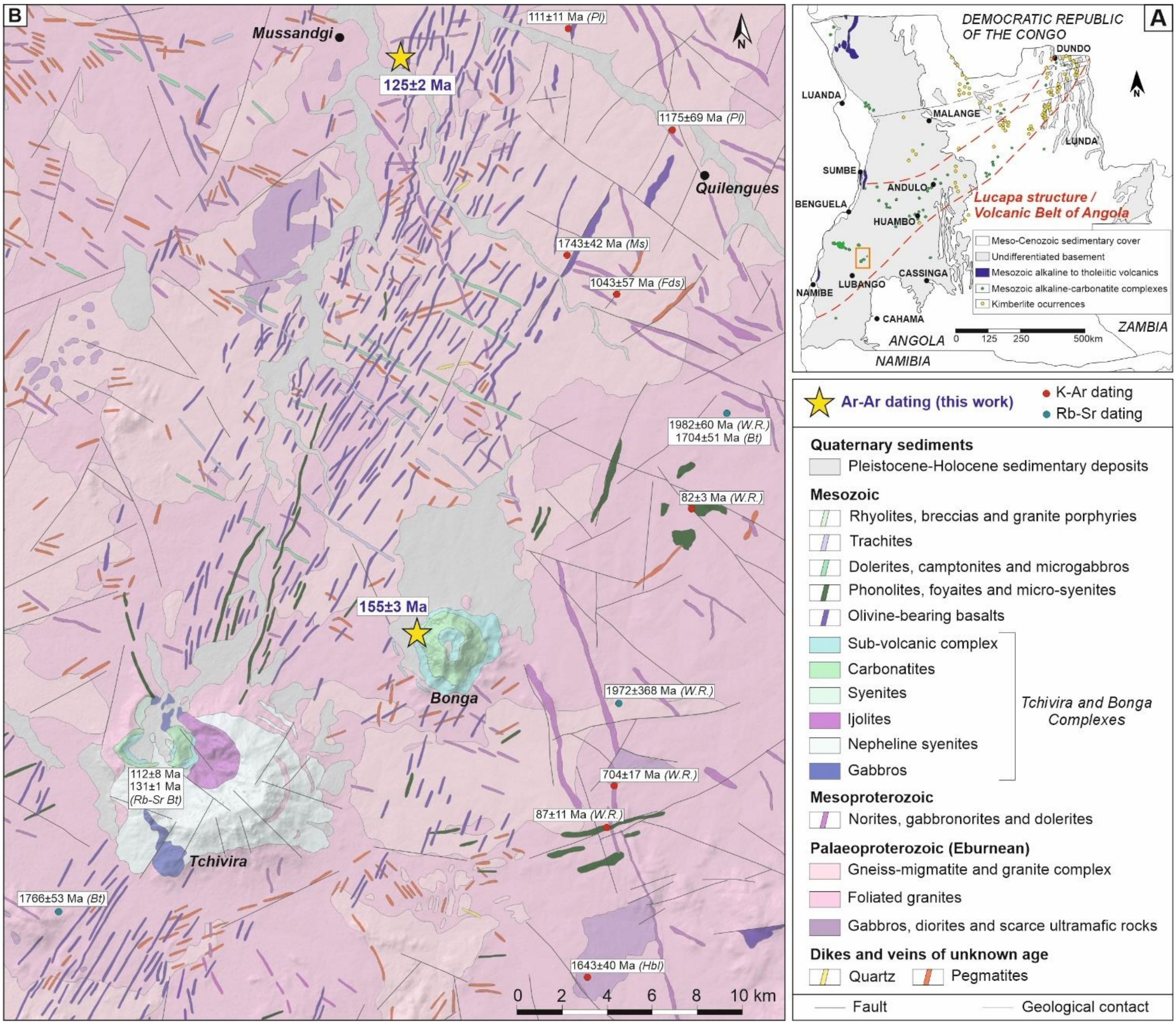

Figure 1. A) Distribution of alkaline-carbonatitic complexes (green), kimberlitic fields (yellow) and alkaline to tholeiitic volcanic materials (dark blue) in Angola, according to Jelsma *et al*. (2013) and Robles Cruz (2013). It is also shown the trace of Mesozoic faults systems related to the Lucapa structure (Lapido-Loureiro, 1968, 1973) or Volcanic Belt of Angola (Machado, 1959). The location of the studied area is highlighted in the orange square. B) Geological map of the studied region (modified from Galán, 2021, and Merino-Martínez, 2022), showing the location of the Tchivira and Bonga alkaline-carbonatitic complexes. Sample location and Ar-Ar dating results from this work are shown in yellow stars. Other Rb-Sr and K-Ar geochronological data from the literature are shown in green and red circles, respectively.

Figura 1. A) Distribución de complejos alcalino-carbonatíticos (verde), campos kimberlíticos (amarillo) y materiales volcánicos alcalinos a toleíticos (azul oscuro) en Angola, según Jelsma *et al*. (2013) y Robles Cruz (2013). También se muestra la traza de sistemas de fallas mesozoicas relacionadas con la estructura de Lucapa (Lapido-Loureiro, 1968, 1973) o Cinturón Volcánico de Angola (Machado, 1959). La localización de la zona estudiada está resaltada en el recuadro naranja. B) Mapa geológico de la región de estudio (modificado de Galán, 2021, y Merino-Martínez, 2022), mostrando la localización de los complejos alcalino-carbonatíticos de Tchivira y Bonga. La localización de las muestras y los resultados de las dataciones Ar-Ar de este trabajo se muestran en estrellas amarillas. Otros datos geocronológicos K-Ar y Rb-Sr de la literatura se indican con círculos rojos y verdes, respectivamente.

A large tholeiitic to alkaline dike swarm (the Mussandgi subvolcanic complex) is also found in the Quilengues area, extending from the village of Mussandgi to the SSW of Tchivira (Fig. 1B). It mainly consists of basalts, phonolites, tinguaites, trachytes, rhyodacites and rhyolitic breccias, which intruded into the Palaeoproterozoic basement in contrasted NNE-SSW and WNW-ESE directions. Some of these subvolcanic materials seem to be intrusive into the Tchivira and Bonga Complexes (Bambi, 2015; Merino-Martínez, 2022). The published K-Ar ages of some basalt and phonolite dikes of the area provided crystallisation ages constrained between 111 and 82 Ma (Silva *et al*., 1973; Torquato, 1977).

3. Analytical methods

$^{40}Ar/^{39}Ar$ dating were performed on mineral separates (hornblende and phlogopite) from two different mafic and/or ultramafic rocks from the Quilengues region. The selected samples were crushed and sieved to obtain fragments ranging in size from 0.1 to 0.5 mm. A hand-held magnet was passed over the samples to remove magnetic minerals and metal fragments/flakes from the grinding process. The samples were rinsed with dilute nitric acid, washed in deionised water, rinsed and then air-dried at room temperature. The minerals were separated by hand, wrapped in aluminium foil and mounted in an irradiation capsule with samples of similar age and neutron flux monitors (Fish Canyon Tuff sanidine, 28.02 Ma; Renne *et al*., 1998). The samples were irradiated at the McMaster Nuclear Reactor in Hamilton, Ontario, for 56 MWH, with a neutron flux of $3x10^{16}$ neutrons/cm^2. Analyses (n=54) of 18 neutron flux monitor positions produced errors of <0.5% in the J value.

The separated minerals were heated at incrementally higher powers in the defocused beam of a 10W CO_2 laser (New Wave Research MIR10) until they fused, in the Noble Gas Laboratory of the Pacific Centre for Isotopic and Geochemical Research, University of British Columbia. The gas developed from each stage was analysed by a VG5400 mass spectrometer equipped with an electronic ion counting multiplier. All measurements were corrected for the total blank system, mass spectrometer sensitivity, mass discrimination, radioactive decay during and after irradiation, as well as air interference from atmospheric contamination and Ca, Cl and K irradiation. The produced isotopic ratios were $(^{40}Ar/^{39}Ar)K = 0.0302$, $(^{37}Ar/^{39}Ar)Ca = 1416.4306$, $(^{36}Ar/^{39}Ar)Ca = 0.3952$, Ca/K = 1.83 ($^{37}ArCa/^{39}ArK$). Plateau and correlation ages were calculated using Isoplot 3.09 software (Ludwig, 2003). Errors are reported at the 2σ level (95% confidence) and are propagated from all sources except the sensitivity of the mass spectrometer and the age of the flow monitor. Tables 1 and 2 summarise the Ar-Ar isotopic results obtained for each analysed sample.

4. Petrographic features of the studied samples

The two samples selected for Ar-Ar dating are a kimberlitic lava flow from the Bonga massif (UTEMD33N087I) and a NNE-trending olivine-bearing basaltic dike (UTEMD33N050I) from the Mussandgi subvolcanic complex (Fig. 1B). The petrographic features of each sample are described below.

4.1. Sample UTEMD33N087I. Kimberlitic lava (Bonga massif)

A 2 meters thick kimberlitic lava flow, apparently coetaneous with the carbonatite magmas from the Bonga carbonatite massif with which it is associated, was chosen for Ar-Ar isotopic analyses. This sample appears as a small tongue of ultramafic rocks between carbonatite breccias found to the northwest of the Bonga massif (Fig. 2A). It shows a brecciated aspect, with a large number of centimetre-sized phenocrysts of phlogopite, pyroxene and olivine, within a dark greyish to greenish microcrystalline matrix (Fig. 2B). It includes fragments of some ultramafic rocks, such as peridotites, pyroxenites and/or hornblendites. Some carbonate crystals are also found in hand sample.

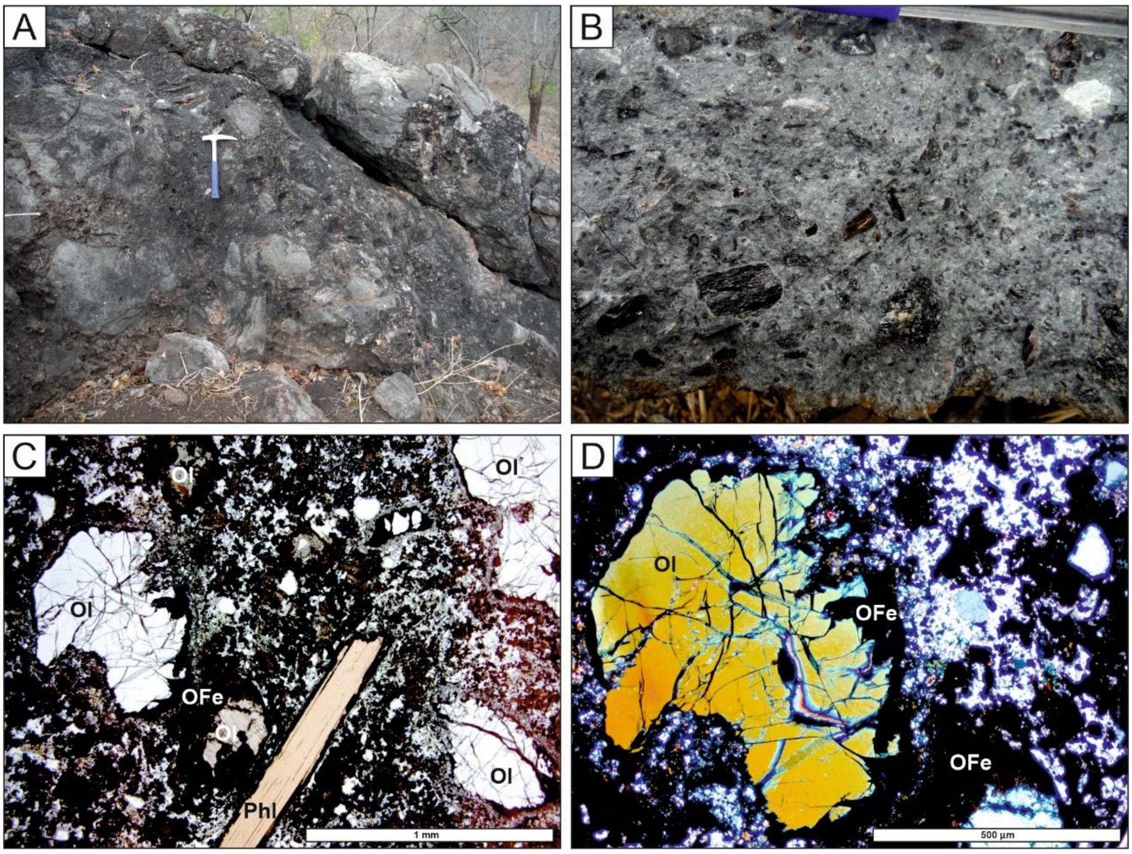

Figure 2. A) Carbonatite breccia to the northwest of the Bonga massif, showing heterometric fragments (up to 30 cm) of eburnean granitoids and calcic carbonatites, surrounded by a medium-grained carbonate matrix. B) Ultramafic rock of kimberlitic appearance, found northwest of the Bonga massif, bearing crystals of various sizes of pyroxene, phlogopite, olivine, carbonates and fragments of ultramafic rocks (dunites, pyroxenites and/or hornblendites). C) Photomicrograph of the kimberlitic rock, showing olivine (Ol) and phlogopite (Phl) phenocrysts, haloed by opaque minerals (OFe), in a micro- to cryptocrystalline matrix, composed of clinopyroxene, olivine, biotite/phlogopite (± amphibole), opaque minerals and carbonate minerals (± plagioclase). D) Detail of the olivine phenocryst (Ol) in cross-polarised light, showing a reaction corona with corroded edges and a halo of opaque minerals (OFe).

Figura 2. A) Brecha carbonatítica al noroeste del macizo de Bonga, mostrando fragmentos heterométricos (de hasta 30 cm) de granitoides eburneanos y carbonatitas cálcicas, rodeados por una matriz carbonatítica de grano medio. B) Roca ultramáfica de aspecto kimberlítico, constituida por cristales de diversos tamaños de piroxeno, flogopita, olivino, carbonatos y fragmentos de rocas ultramáficas (dunitas, piroxenitas y/o hornblenditas), encontrada al noroeste del macizo de Bonga. C) Microfotografía de la roca kimberlítica, mostrando fenocristales de olivino (Ol) y flogopita (Phl) , aureolados por minerales opacos (OFe), en una matriz micro a criptocristalina, compuesta por clinopiroxeno, olivino, biotita/flogopita (± anfíbol), minerales opacos y minerales carbonatados (± plagioclasa). D) Detalle del fenocristal de olivino (Ol) en nícoles cruzados, mostrando una corona de reacción con bordes corroidos y un halo de minerales opacos (OFe).

Under the microscope, this sample is a holocrystalline (sub-)volcanic rock with porphyritic texture. Subidio- to allotriomorphic phenocrysts (up to 1 cm) of olivine, clinopyroxene, phlogopite-biotite, opaque minerals and chromite, together with some metallic sulphides are distinguished in thin section (Figs. 2C and D). All phenocrysts show corroded edges and present a reaction halo composed of opaque minerals, indicating disequilibrium reactions during mineral crystallisation. Rock-forming minerals do not show a preferential flow direction, although some phlogopite and biotite crystals seem to be aligned following a common pattern. The fine-grained microcrystalline matrix is composed of clinopyroxene, olivine, biotite/phlogopite (± amphibole), opaque minerals and carbonates (± plagioclase).

4.2. Sample UTEMD33N050I. Basalt dike (Mussandgi subvolcanic complex)

A basaltic sample was taken 26 km to the north of the Bonga Complex, from the northern segment of the NNE-SSW dike swarm of the Mussandgi complex. Similar basaltic samples have been found intruding syenite materials from the Tchivira Complex (Fig. 3A). This rock exhibits a porphyritic and vacuolar texture, composed of small phenocrysts of olivine, pyroxene and amphibole, up to 2 mm in size, within a dark fine matrix (Fig. 3B). The vacuoles are filled with radial zeolite-type minerals (± carbonates), low-temperature amphiboles (actinolite-tremolite) and a large amount of metallic sulphides (pyrite, chalcopyrite, galena, among others).

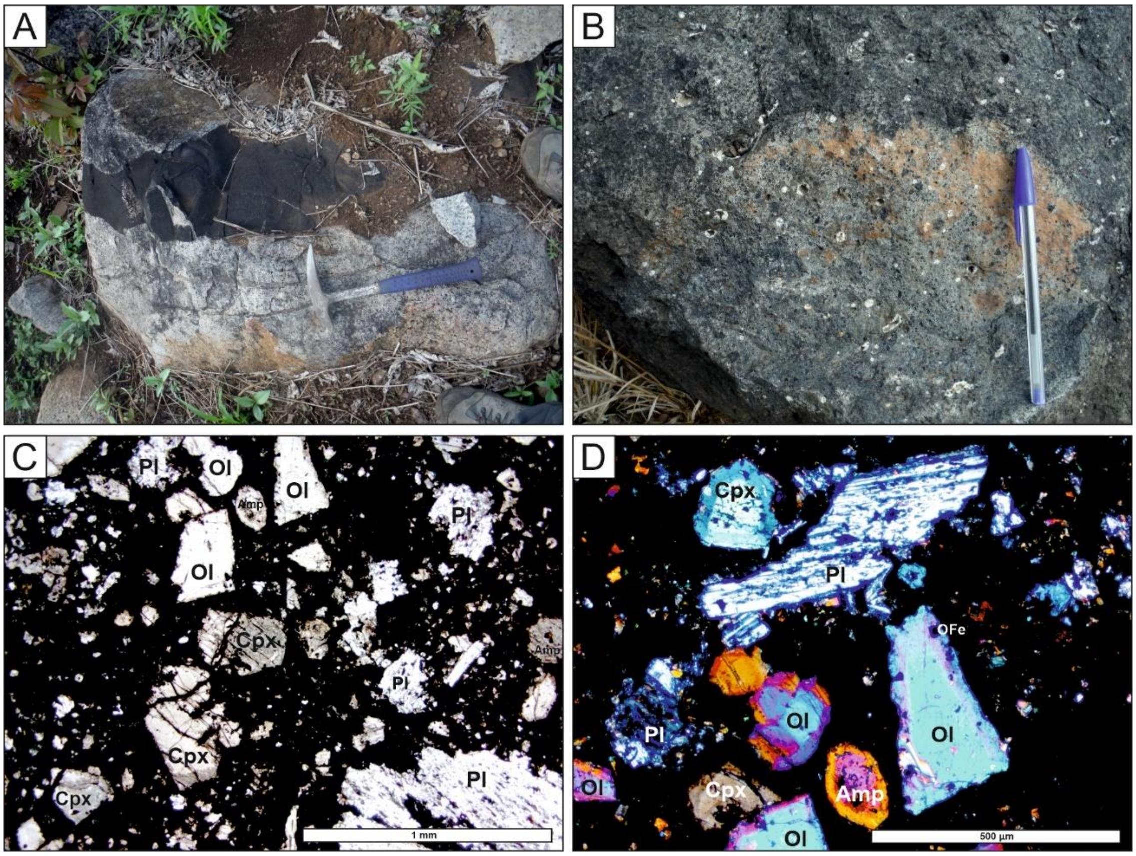

Figure 3. A) Dolerite dike intrusive into syenitic facies of the Tchivira Complex in NNE-SSW direction. B) NNE-SSW trending pyroxene- and olivine-bearing basalt dike, showing vacuoles filled by metallic sulphides, zeolites, carbonates and other secondary minerals. C) Microphotograph of the basalt dike showing phenocrysts of plagioclase (Pl), clinopyroxene (Cpx), olivine (Ol) and amphibole (Amp) within a micro- to cryptocrystalline matrix. D) Detail of the polysynthetic twinning of the plagioclase phenocrysts (Pl) in cross-polarised light, the zoning of the pyroxene (Cpx) and amphibole (Amp) crystals and the halo of opaque minerals (OFe) surrounding the phenocrysts.

Figura 3. A) Dique de dolerita intrusivo en facies sieníticas del Complejo Tchivira en dirección NNE-SSW. B) Dique de basalto piroxénico-olivínico, de tendencia NNE-SSW, mostrando vacuolas rellenas por sulfuros metálicos, zeolitas, carbonatos y otros minerales secundarios. C) Microfotografía del dique basáltico mostrando fenocristales de plagioclasa (Pl), clinopiroxeno (Cpx), olivino (Ol) y anfíbol (Amp) dentro de una matriz micro a criptocristalina. D) Detalle del maclado polisintético de los fenocristales de plagioclasa (Pl) con nícoles cruzados, la zonación de los cristales de piroxeno (Cpx) y anfíbol (Amp) y el halo de minerales opacos (OFe) que rodea a los fenocristales.

Under the microscope, the sample shows a holocrystalline porphyritic texture (Fig. 3C). It contains idio- to sub-idiomorphic phenocrysts of plagioclase and clinopyroxene (augite), up to 5 mm in size, some phenocrysts of olivine and amphibole, and more scarcely, smaller opaque minerals (< 1 mm). Plagioclase, partially altered to sericite, and augite phenocrysts show normal zoning. Some hornblende crystals are surrounded by a halo of opaque minerals which, together with the corroded edges shown in other main minerals (e.g., plagioclase, olivine, augite), indicate instability processes or mineral disequilibrium with the melt (Fig. 3D). Some prismatic plagioclase phenocrysts are oriented in a preferred direction, although no other magmatic flow patterns have been identified in the thin section. The micro- to cryptocrystalline matrix is primarily composed of opaque, with accessory plagioclase, pyroxene, olivine, and amphibole (Figs. 3C and D).

5. Ar-Ar geochronological results

The Ar-Ar radiometric results obtained on phlogopite separates of the kimberlitic lava from the Bonga carbonatite massif (sample UTEMD33N087I) show no evidence of ^{40}Ar excess (Table 1). The Ar-Ar plateau diagram presents an almost continuous spectra from the third step to the end of the profile, which gave an Ar-Ar plateau age of 155.2 ± 2.9 Ma (MSWD = 0.47, probability = 0.83; Fig. 4A). The two first low-temperature steps, which displayed an average age of 258.5 ± 56 Ma, are probably derived from ^{39}Ar recoil in the sample during laboratory rock heating and irradiation, as suggested by the low ^{39}Ar (1.21-6.75 %) and K/Ca ratios (10.20-22.62) contents (Table 1). ^{40}Ar-^{39}Ar dating often shows high apparent ages in the initial Ar heating steps, approaching to the most real age of the sample with progressive release of ^{39}Ar (e.g., Renne *et al*., 1996; Kelley, 2002). The confidence of the reported Ar-Ar plateau age is reinforced by the calculated inverse isochron age, which yields a similar age of 150.3 ± 5.8 Ma (MSWD = 0.36; Fig. 4A), as well as that obtained for the normal isochron age (150.2 ± 5.8 Ma; MSWD = 0.33; not shown). Hence, the Ar-Ar plateau age of 155.2 ± 2.9 Ma is considered as the most reliable age for the intrusion of the kimberlitic lava in the Bonga massif.

UTEMD33N087I Phlogopite															
Laser	*Isotope Ratios*														
Power (%)	*^{40}Ar/^{39}Ar*	*2s*	*^{36}Ar/^{39}Ar*	*2s*	*^{39}Ar/^{40}Ar*	*2s*	*^{36}Ar/^{40}Ar*	*2s*	*Rho*	*K/Ca*	*%^{40}Ar rad*	*f^{39}Ar*	*^{40}Ar*/ ^{39}ArK*	*Age (Ma)*	*2s*
2.3	73.23	17.92	0.067	0.017	0.014	0.003	0.00092	0.00029	0.604	10.20	72.56	1.21	53.136	261.50	± 80.54
2.7	69.48	6.49	0.059	0.009	0.014	0.001	0.00085	0.00015	0.469	22.62	74.61	6.75	51.837	255.53	± 31.42
3.1	46.51	2.00	0.049	0.006	0.022	0.001	0.00106	0.00013	0.312	1039.41	68.27	10.19	31.753	160.72	± 12.26
3.7	43.06	0.99	0.041	0.002	0.023	0.001	0.00096	0.00006	0.207	145.66	71.33	28.27	30.714	155.67	± 5.34
3.7	39.33	5.49	0.022	0.004	0.025	0.004	0.00056	0.00013	0.535	93.98	83.24	4.04	32.739	165.49	± 26.70
4.1	40.85	4.54	0.030	0.008	0.024	0.003	0.00074	0.00020	0.386	101.57	77.78	4.10	31.775	160.82	± 24.31
5.1	32.99	1.05	0.009	0.001	0.030	0.001	0.00028	0.00003	0.212	472.88	91.57	17.69	30.210	153.22	± 5.13
6.1	38.22	1.57	0.024	0.004	0.026	0.001	0.00062	0.00010	0.155	1558.3	81.55	12.23	31.174	157.91	± 8.85
7.5	36.33	1.16	0.020	0.002	0.028	0.001	0.00055	0.00005	0.268	192.13	83.49	15.51	30.330	153.81	± 5.99

J = 0.00289010 ± 0.00000578   Volume ^{39}ArK = 0.064 x E^{-13} cm^3 NPT

Integrated Date = 156.13 ± 2.83 Ma

Plateau age = 155.2 ± 2.9 Ma   (2s, including J-error of .4%)   MSWD = 0.47, probability=0.83   Includes 92% of the ^{39}Ar   steps 3 through 9

Inverse isochron (correlation age) results: Model 1 Solution (±95%-conf.) on 7 points

Age = 150.3 ± 5.8 Ma   Initial ^{40}Ar/^{36}Ar =321 ± 42   MSWD = 0.36   Probability = 0.88

Table 1. Ar-Ar isotopic results on phlogopite from the studied kimberlitic lava flow of the Bonga Complex (UTEMD33N087I).

Tabla 1. Resultados isotópicos de Ar-Ar en flogopita de la muestra de colada kimberlítica estudiada del Complejo de Bonga (UTEMD33N087I).

The Ar-Ar results acquired on hornblende separates from the NNE-SSW trending basaltic dike of the Mussandgi subvolcanic complex (sample UTEMD33N050I) also show little evidence of Ar disturbance (Table 2). With the exception of the first step (Fig. 4B), which provided an older Ar-Ar age of 181.6 ± 37.8 Ma, probably derived from the low ^{39}Ar (2.08%) and radiogenic ^{40}Ar (16.29 %) contents and high ^{40}Ar/^{39}Ar ratios (221.47), the whole age data are constrained between 134.4 and 120.8 Ma (Table 2). Nevertheless, steps two to six display a slightly increasing staircase age spectra, presumably associated with their high ^{40}Ar/^{39}Ar (136.3-36.15) ratios, and are not considered for age calculations. The last four steps define a fairly continuous plateau and are selected for determine the age of this sample. Therefore, an Ar-Ar plateau age of 124.7 ± 2.2 Ma (MSWD = 0.29, probability = 0.83; Fig. 4B) reveals the crystallisation age of the basaltic magma. This age is consistent with those calculated from the inverse isochron age (124.5 ± 4.4 Ma; MSWD = 2.4) and the normal isochron age (124.1 ± 4.2 Ma; MSWD = 2.3) of the whole dataset (excluding the first step), suggesting a high level of confidence in the calculated age data.

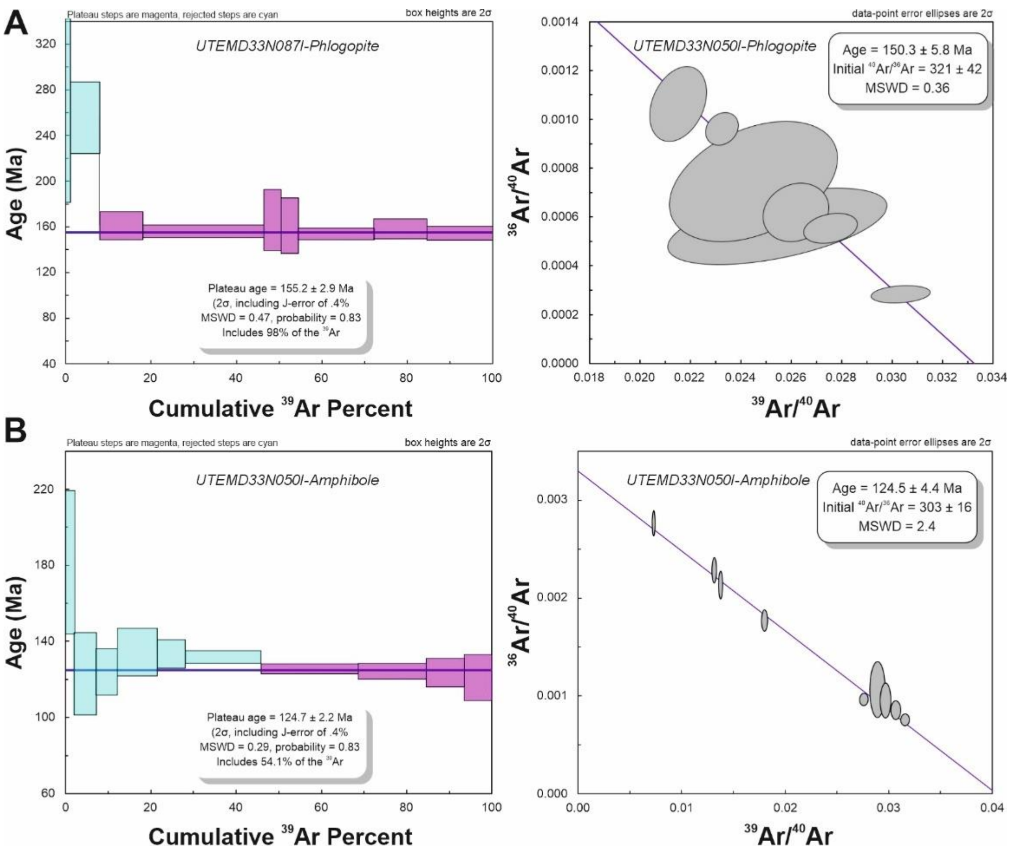

Figure 4. A) Ar-Ar plateau age (155.2 ± 2.9 Ma; left) and inverse isochron age (150.3 ± 5.8 Ma; right) obtained from phlogopite separates of the kimberlitic lava flow to the northwest of the Bonga massif (sample UTEMD33N087I). B) Ar-Ar plateau age (124.7 ± 2.2 Ma; left) and inverse isochron age (124.5 ± 4.4 Ma; right) obtained from amphibole separates from a basaltic dike of the Mussandgi complex (sample UTEMD33N050I).

Figura 4. A) Edad plateau Ar-Ar (155.2 ± 2.9 Ma; izquierda) y edad isócrona inversa (150.3 ± 5.8 Ma; derecha) obtenidas en los separados de flogopita de la colada de lava kimberlítica al noroeste del macizo de Bonga (muestra UTEMD33N087I). B) Edad plateau Ar-Ar (124.7 ± 2.2 Ma; izquierda) y edad isócrona inversa (124.5 ± 4.4 Ma; derecha) obtenidas en separados de anfíbol de un dique basáltico del complejo de Mussandgi (muestra UTEMD33N050I).

UTEMD33N050I Hbl															
Laser	*Isotope Ratios*														
Power (%)	*$^{40}Ar/^{39}Ar$*	*2s*	*$^{36}Ar/^{39}Ar$*	*2s*	*$^{39}Ar/^{40}Ar$*	*2s*	*$^{36}Ar/^{40}Ar$*	*2s*	*Rho*	*K/Ca*	*%^{40}Ar rad*	*$f^{39}Ar$*	*$^{40}Ar^*/^{39}ArK$*	*Age (Ma)*	*2s*
2.3	221.47	3.75	0.62	0.028	0.005	0.0001	0.0028	0.0001	0.030	0.40	16.29	2.08	36.101	181.57	± 37.81
2.7	136.29	2.11	0.38	0.016	0.007	0.0001	0.0028	0.0001	0.006	0.21	17.61	5.10	24.050	122.94	± 21.62
3	75.69	1.02	0.17	0.008	0.013	0.0002	0.0023	0.0001	0.013	0.16	31.98	4.92	24.264	124.00	± 12.17
3.6	72.37	0.86	0.15	0.009	0.014	0.0002	0.0021	0.0001	0.012	0.41	36.4	9.33	26.371	134.38	± 12.49
4	55.35	0.76	0.10	0.005	0.018	0.0002	0.0018	0.0001	0.009	0.43	47.19	6.66	26.142	133.26	± 7.55
5	36.15	0.45	0.04	0.002	0.028	0.0003	0.0010	0.0001	0.048	0.32	71.35	17.80	25.824	131.69	± 3.34
6	31.50	0.35	0.03	0.002	0.032	0.0004	0.0007	0.0000	0.008	0.10	77.62	22.63	24.546	125.39	± 2.71
7	32.00	0.39	0.04	0.002	0.031	0.0004	0.0008	0.0001	0.006	0.02	74.63	16.06	24.293	124.15	± 4.11
8	31.80	0.39	0.06	0.003	0.030	0.0004	0.0009	0.0001	0.003	0.01	71.73	8.85	24.126	123.32	± 7.48
9	31.35	0.47	0.08	0.005	0.029	0.0006	0.0011	0.0002	0.005	0.00	68.40	6.56	23.623	120.83	± 12.18

J = 0.00288860 ± 0.00000578   Volume $^{39}ArK = 0.102 \times E^{-13}$ cm^3 NPT

Integrated Date = 127.27 ± 1.71 Ma

Plateau age = 124.7 ± 2.2 Ma   (2s, including J-error of .4%)   MSWD = 0.29, probability=0.83   Includes 54.1% of the ^{39}Ar steps 7 through 10

Inverse isochron (correlation age) results: Model 1 Solution (±95%-conf.) on 9 points

Age = 124.5 ± 4.4 Ma   Initial $^{40}Ar/^{36}Ar$ =303 ± 16   MSWD = 2.4   Probability = 0.02

Table 2. Ar-Ar isotopic results on hornblende from the studied basaltic dike (UTEMD33N050I).

Tabla 2. Resultados isotópicos de Ar-Ar en hornblenda de la muestra de dique basáltico estudiado (UTEMD33N050I).

6. Discussion

6.1. Intrusion age of the studied samples and temporal relationships

The field and structural relationship between the kimberlitic materials and the carbonatite breccias of the Bonga massif (Figs. 2A and 2B) suggest that they intruded contemporaneously with the carbonatite magmas. The Ar-Ar plateau age obtained for the kimberlitic lava flow of the Bonga massif indicates a crystallisation age of 155.2 ± 2.9 Ma (Fig. 4A), indicating a similar age intrusion for the Bonga Complex. Nevertheless, Torquato (1977) and Cahen *et al*. (1984) report K-Ar ages of syenitic to ijolitic rocks from the Tchivira Complex of 126 ± 4 Ma and between 130 and 138 Ma, while Vale *et al*. (1972) and Allsopp & Hargraves (1985) obtained Rb/Sr ages for the intrusion of the nepheline syenites of Tchivira of 112 ± 8 and 131 ± 1 Ma, respectively. This variation in the crystallisation ages of alkaline and ultrapotassic magmas could indicate that emplacement of the Tchivira and Bonga Complexes was not synchronous and took place over a long time period (155-112 Ma). On the other hand, this age variation could be evidencing the influence of hydrothermal and/or metasomatic processes and thermal impacts associated with the different episodes of intrusion of the alkaline-carbonatite magmas (e.g., Bambi, 2015), promoting isotope disturbances in the system and inducing younger ages for the crystallisation of the Tchivira Complex. In any case, it is clear that the kimberlitic lavas found in the Bonga Complex are closely related to the intrusion of the alkaline and carbonatitic magmas described above, and may testify to a slightly older magmatic episode, of upper Jurassic age (155 Ma), than previously assessed to the Tchivira Complex (138-112 Ma; lower Cretaceous).

The field relationships between the set of basaltic and alkaline dikes and the Tchivira and Bonga alkaline-carbonatite massifs suggest different temporal constraints. Although there are no clear structural relationships between the alkaline to tholeiitic dikes and the carbonatitic Bonga Complex, some syenite facies of the Tchivira Complex are evidently intruded by dolerite materials alike to those found in the Mussandgi subvolcanic complex (Fig. 3A). The Ar-Ar plateau age obtained from the basaltic dike found to the north of the Bonga Complex indicates an intrusion age of 124.7 ± 2.2 Ma (Fig. 4B). This age is similar, within error, to the K-Ar age in plagioclase reported in another NNE-SSW trending basalt dike in the surrounding area (111 ± 11 Ma; Fig. 1; Silva *et al*., 1973). Other basaltic and dolerite dikes to the east and north of Quipungo were also dated between 132 ± 13 Ma and 126 ± 2.2 Ma using whole-rock K-Ar and Rb-Sr on biotite dating, respectively (Figs. 1B and 5; Mendes, 1968; Silva *et al*., 1973; Torquato, 1977). Although these latter K-Ar and Rb-Sr ages are almost indistinguishable within error, the high consistency between the $^{40}Ar/^{39}Ar$ plateau/isochron ages indicates that the Ar/Ar method and reported results are more reliable than those obtained by the other dating methods (e.g., Kelley, 2002). Thus, the age data suggest a time spam between 132 and 111 Ma for the intrusion of the tholeiitic materials in the region.

Summarising, these data suggest that tholeiitic to bimodal and alkaline-carbonatitic magmatism occurred in distinct stages during the fragmentation of Pangea, in a long period of intraplate magmatism during the Mesozoic. Hence, the whole age dataset here presented imply the ascent of mantle-derived melts along crustal fractures during the Lower Cretaceous, after the Upper Jurassic to Lower Cretaceous emplacement of the Tchivira and Bonga alkaline-carbonatitic complexes.

6.2. Mesozoic alkaline-carbonatitic and tholeiitic magmatism in SW Angola and counterparts

Several studies described a magmatic period constrained between 138 and 130 Ma for the intrusion of the diverse alkaline-carbonatite massifs in Angola, based on Rb/Sr isochron dating (Cahen *et al*., 1984; Allsopp & Hargraves, 1985), related to the breakup of Gondwana and the opening of the Atlantic Ocean during the Mesozoic (Issa Filho *et al*., 1991). However, Jelsma *et al*. (2013) report U-Pb ages in kimberlitic rocks from central Angola (Lubia cluster) between 252 and 216 Ma (Fig. 5), indicating an episode of ultrapotassic magmatism during the Late-Permian to Triassic period. Similar whole-rock K-Ar and Ar-Ar ages between 222 and 210 Ma are reported in basaltic lava flows found in the Kwanza Basin (Torquato & Amaral, 1973; Merino-Martínez *et al.,* 2021), possibly related to the preliminary stages for the formation of the Central Atlantic Magmatic Province (204-192 Ma; Svensen *et al*., 2017; Oliveira *et al*., 2023). Other $^{40}Ar/^{39}Ar$ data of the African Karoo Continental Flood Basalts in Namibia, Botswana and Zambia are constrained between 185-170 Ma (Fig. 5; Jourdan *et al*., 2007). These ages are much older than that obtained in this study for the kimberlitic magma from the carbonatitic Bonga massif (155.2 ± 2.9 Ma; Fig. 4A), and therefore, related to distinct episodes of magmatism. Our age coincides with the whole-rock K-Ar ages reported in basalts and dolerites from the Sumbe area (168-140 Ma; Torquato *and* Amaral, 1973; Torquato, 1977). These findings possibly suggest a mantle-derived magmatism in an incipient rifting phase promoted by the assistance of plume-induced lithospheric weakening, related to the emplacement of alkaline-carbonatitic bodies in central-western Angola at late Jurassic times.

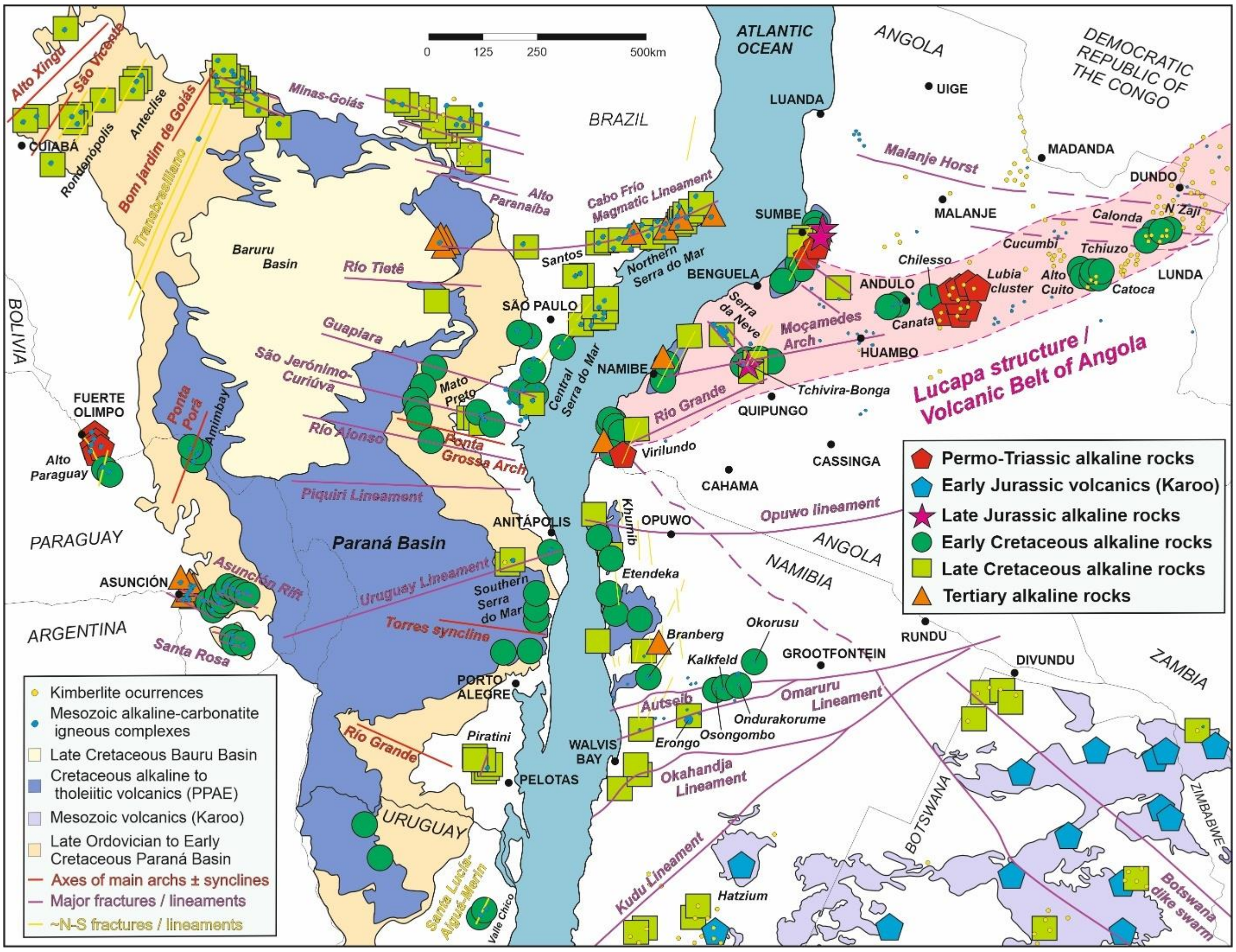

Figure 5. Distribution of alkaline, carbonatitic and kimberlitic complexes and alkaline to tholeiitic magmatic provinces of southwestern Africa and of the Paraná Basin from central-southeastern Brazil, showing their relationships with major structures and crustal lineaments (modified from Comin-Chiaramonti *et al*., 2005; Riccomini *et al*., 2005; Bambi *et al*., 2015; Corner & Durrheim, 2018, and references cited in these works).

Figura 5. Distribución de los complejos alcalinos, carbonatíticos y kimberlíticos y de las provincias magmáticas alcalinas a toleíticas de África sudoccidental y de la cuenca del Paraná del centro-sureste de Brasil, mostrando sus relaciones con las principales estructuras y lineamientos corticales (modificado de Comin-Chiaramonti *et al*., 2005; Riccomini *et al*., 2005; Bambi *et al*., 2015; Corner & Durrheim, 2018, y referencias citadas en estos trabajos).

Nonetheless, Jelsma *et al.* (2013) also reported a U-Pb age of 124 Ma in a carbonatitic rock from central Angola (the Chilesso carbonatite; Fig. 5), also evidencing distinct episodes of alkaline to carbonatitic magmatism recorded in the Mesozoic. Most kimberlites from northeastern Angola have been dated at between 145 and 113 Ma (Robles-Cruz *et al*., 2012; Castillo-Oliver *et al*., 2016). Indeed, Jelsma *et al*. (2004, 2009) and Robles-Cruz (2013) suggest that alkaline magmas of Aptian age (ca. 120 Ma) are associated with a NE-SW tectonic direction, coincident with the Lucapa structure and other kimberlitic and alkaline-carbonatitic lineaments found in the São Francisco, Kaapvaal and Congo-Kasai cratons (Da Costa, 2008; Batumike *et al*., 2009; Jelsma *et al*., 2009), emplaced in a state of incipient rifting.

Given the spatio-temporal relationship between the carbonatite massifs and alkaline to tholeiitic dikes of Angola, this magmatism should be consider contemporaneous with other tholeiitic basalts (133-129 Ma) and alkaline-potassic magmas (147-126 Ma) found in the eastern region of Paraguay (Comin-Chiaramonti *et al*., 1999; Renne *et al.*, 1996), the alkaline-carbonatite complexes from Anitápolis and the Ponta Grossa Arc (138-128 Ma) of southern Brazil (Amaral *et al*., 1967; Morbidelli *et al*., 1995; Comin-Chiaramonti *et al*., 2005), and alkaline-carbonatite complexes in northwest Namibia (i.e., Osongombo, Kalkfeld, Ondurakorume, Okorusu, 137-124 Ma; Fig. 5, Milner *et al*., 1995; Le Roex & Lanyon, 1998), all related to the opening of the Atlantic Ocean. In fact, the Ar-Ar plateau age obtained from the basaltic dike of the Mussandgi Complex (124.7 ± 2.2 Ma; Fig. 4B) is coeval wit the K-Ar ages from 132 Ma to 126 Ma obtained in tholeiitic dolerite dikes from the Sumbe area and other Ar-Ar ages between 132-120 Ma obtained from mineral separates of diverse volcanic rocks from the Namibe basin, in the coastal region of western Angola (Torquato & Amaral, 1973; Renne *et al*., 1996; Marzoli *et al*., 1999; Escuder-Viruete *et al*., 2021). Hence, the intrusion of these mafic dikes is related to the progress of crustal rifting and the opening of the South Atlantic Ocean. They could represent the feeding sources of the upwelled mantle-derived melts that extruded in the form of LIPs, which gave rise to the Paraná-Angola-Etendeka Province, preceding the oceanisation and the opening of the Atlantic Ocean.

It is important to highlight that other WNW-ESE to ENE-WS trending phonolite dikes cropping out in the Quipungo region have been dated between 87 and 82 Ma by whole-rock K-Ar dating (Figs. 1 and 5; Silva *et al*., 1973). Distinct authors highlight that younger alkaline complexes of Santonian age (ca. 85 Ma), such as those found in the Republic of Congo (Mbuji-Mayi kimberlites; Schärer *et al*., 1997), are aligned according to a different tectonic direction (following an ~E-W direction); which suggests an intrusion of alkaline magmas in a second period associated with the progress of rifting and the action of deep transform faults (Jelsma *et al*., 2004, 2009; Robles-Cruz, 2013). These patterns are orthogonal to the lineaments found in Late Cretaceous kimberlites from southern Namibia to Zambia (Moore *et al*., 2008; Farr *et al*., 2018), and are related to a phase of subsidence of the Congo Basin from 110 to 60 Ma (Linol *et al*., 2015). Allsopp & Hargraves (1985) reported a Rb-Sr age of 104 ± 1 Ma in nepheline syenites from the Serra da Neve, slightly younger than that assigned to the massifs of Tchivira (138-112 Ma; Vale *et al.*, 1972; Allsopp & Hargraves, 1985), Bonga (155 ± 3 Ma; this study), or Canata (Ar-Ar ages of 130-124 Ma; Jelsma *et al*., 2013; Escuder-Viruete & Gumiel, 2021). Other K-Ar and Ar-Ar ages reported for tholeiitic and alkaline magmas in the Kwanza Basin are constrained between 105 and 84 Ma (Torquato & Amaral, 1973; Torquato, 1977; Marzoli *et al*., 1999). These ages agree with the two magmatic pulses described by Torsvik *et al.* (2009) during the Cretaceous, related to the rifting and subsequent drifting between South America and Africa.

As a whole, the isotope age data reported in the literature and the Ar-Ar ages presented in this work indicate a broad intracontinental magmatic period between 252 and 84 Ma, suggesting distinct periods of bimodal magmatism associated with the crustal breakup and progressive Atlantic rifting during Mesozoic times (Svensen *et al.,* 2017).

7. Conclusions

The newly acquired Ar-Ar radiogenic dating performed during the PLANAGEO project have improved the geochronological knowledge for the emplacement of distinct alkaline to tholeiitic intrusive bodies in SW Angola. The Ar-Ar plateau ages obtained in mineral separates (phlogopite and amphibole) from a kimberlitic lava flow (155.2 ± 2.9 Ma), presumably contemporaneous to the Bonga carbonatite massif, and from a NNE-SSW trending basaltic dike of the Quipungo region (124.7 ± 2.2 Ma), reveal separate magmatic episodes related to the opening of the South Atlantic Ocean. The calculated plateau ages for both samples are indistinguishable from the isochron ages at the 2σ level, thereby confirming the validity of the reported Ar-Ar dating. This magmatism is coeval to the extrusion of other volcanic rocks found in the coastal region of Angola, suggesting a broad geodynamic relationship.

The available geochronological data from SW Angola and its counterparts suggest a wide time interval (i.e., 252-84 Ma) for the alkaline-carbonatitic and extrusive bimodal magmatism. These contrasting intrusion ages are controlled by different stages of the continental rifting and subsequent drifting between Africa and America. The spatio-temporal relationships between the recorded emplacement ages and the lineaments of alkaline-carbonatitic and bimodal rocks suggest a structural control on the intrusion of these magmas during a long period of intraplate Mesozoic magmatism. The intrusive bodies displaying NE-SW and NNE-SSW directions, almost parallel to the coast and the mid-oceanic Atlantic ridge, mark the initial stages of rifting; while the ~E-W striking bodies would be related to the more evolved stages of the opening process (drifting), with the intrusion of bimodal magmas along fracture planes generated by the transcurrent movements during the progress of opening.

Acknowledgments

This work is a result of the National Geological Plan of Angola (PLANAGEO). This project was supported by the Government of the Republic of Angola and implemented by the Geological Survey of Angola (IGEO), under the oversight of the Angolan Ministry of Mineral Resources, Oil and Gas (MIREMPET). We would like to express our gratitude for the invaluable assistance provided by the local staff, specially to our colleague José Cipriano Miguel, who facilitated the challenging conditions during our fieldwork and geological sampling. A special mention goes to our colleague Gustavo Galán, who left us before the end of the project, and his inclusion as co-author of this article is a recognition of his mapping work in the Quipungo region. We also highly appreciate the precious contribution of the staff of Impulso Industrial Alternativo to this project. The authors are also grateful for the invaluable contributions to the refinement of the article's content by Professor Ramón Casillas and an anonymous reviewer, and for the commendable efforts and professional expertise of the guest editor Elsa Ramalho.

Authorship contribution statement

Enrique Merino-Martínez: Writing - Original Draft, Conceptualization, Investigation, Methodology, Data Curation, Formal analysis, Visualization, Writing - Review & Editing, Validation, Project administration, Supervision.
Pablo Valverde-Vaquero: Investigation, Data Curation, Investigation, Methodology, Resources, Formal Analysis, Validation, Writing - Review & Editing.
Aratz Beranoaguirre: Investigation, Data Curation, Resources, Formal Analysis.
Gustavo Galán: Investigation.
Janet Gabites: Resources, Formal analysis, Data Curation, Resources.
José Manuel: Supervision, Project administration, Funding acquisition.

References

Alberti, A., Castorina, F., Censi, P., Comin-Chiaramonti, P., & Gomes, C. B. (1999). Geochemical characteristics of Cretaceous carbonatites from Angola. Journal of African Earth Sciences, 29(4), 735-759.

Alberti A., Piccirillo, E. M., Bellieni, G., Civetta, L., Comin-Chiaramonti, P., & Morais, E. A. A. (1992). Mesozoic acid volcanics from southern Angola: petrology, Sr-Nd isotope characteristics and correlation with the acid stratoid volcanic suites of the Paranà basin (south-eastern Brazil). European Journal of Mineralogy, 4, 597-604.

Allsopp, H., & Hargraves, R. (1985). Rb-Sr ages and palaeomagnetic data for some Angolan alkaline intrusives. Transactions of the Geological Society of South Africa, 88, 295-299.

Amaral, G., Bushee, J., Cordani, U. G., Kawashita, K., & Reynolds, J. H. (1967). Potassium-argon ages of alkaline rocks from southern Brazil. Geochimica et Cosmochimica Acta, 31(2), 117-142.

Bambi, A. C. J. M. (2015). Metalogenia de las carbonatitas en domínios plutónicos, subvolcánicos y volcánicos: Tchivira, Bonga y Catanda, Angola. PhD Thesis, Universitat de Barcelona, 705 p.

Batumike, J. M., Griffin, W. L., O´Reilly, S. Y., Belousova, E. A., & Pawlitschek, M. (2009). Crustal evolution in the Central Congo-Kasai Craton. Luebo, D.R., Congo: Insights from zircon U-Pb ages, Hf-isotope and trace element data. Precambrian Research, 170(1-2), 107-115.

Cahen, L., Snelling, N. J., Delhal, J., & Vail, J. R. (1984). The geochronology and evolution of Africa: London, Oxford University Press, 512 p.

Carvalho, H. (1982). Carta Geológica de Angola, à escala 1:100.000.. Instituto Investigação Científica Tropical (Centro Geologia), Lisbon.

Carvalho, H. (1983). Notice explicative prèliminaire sur la géologie d'Angola. Garcia de Orta, 6 (1/2), 15-30.

Castillo-Oliver, M., Galí, S., Melgarejo, J. C., Griffin, W. L., Belousova, E., Pearson, N. J., Watangua, M., & O'Reilly, S. Y. (2016). Trace-element geochemistry and U–Pb dating of perovskite in kimberlites of the Lunda Norte province (NE Angola): Petrogenetic and tectonic implications. Chemical Geology, 426, 118-134.

Coltorti, M., Alberti, A., Beccaluva, L., Dos Santos, A. B., Mazzucchelli, M., Morais, E., Rivalenti, G., & Siena, F. (1993). The Tchivira Bonga alkaline-carbonatite complex (Angola): petrological study and comparison with some Brazilian analogues. European Journal of Mineralogy, 5, 1001-1024.

Comin-Chiaramonti, P., Barros Gomes, C., Cundari, Al., Castorina, F., & Censi, P. (2007). A review of carbonatitic magmatism in the Paraná-Angola-Namibia (PAN) system. Periodico di Mineralogia, 76(2-3), 25-78.

Comin-Chiaramonti, P., Cundari, A., De Graff, J. M., Gomes, C. B., & Piccirillo, E. M. (1999). Early Cretaceous-Tertiary magmatism in Eastern Paraguay (western Paraná basin): Geological, geophysical and geochemical relationships. Journal of Geodynamics, 28, 375-391.

Comin-Chiaramonti, P., Gomes, C. B., Censi, P., & Speziale, S. (2005). Carbonatites from southeastern Brazil: a model for the carbon and oxygen isotope variations. In: Comin-Chiaramonti, P., Gomes, C.B. (eds): Mesozoic to Cenozoic alkaline magmatism in the Brazilian platform. Edusp Fapesp, São Paulo, Brazil, pp. 629-650.

Corner, B., & Durrheim, R. J. (2018). An Integrated Geophysical and Geological Interpretation of the Southern African Lithosphere. In: Siegesmund et al. (eds.), Geology of Southwest Gondwana. Regional Geology Reviews, pp. 19-61. https://doi.org/10.1007/978-3-319-68920-3_2

Da Costa, G. V. (2008). Química mineral e geotermobarometria de xenólitos mantélicos do kimberlito Canastra-01. PhD Thesis, Instituto de Geociências, Universidade de Brasília, 137 p.

Ernst, R. E., & Bell, K. (2010). Large igneous provinces (LIPs) and carbonatites. Mineralogy and Petrology, 98, 55-76.

Escuder-Viruete, J., Correia, J., & Quintana, L. (2021). Mapa geológico e Notícia explicativa da carta geológica de Namibe. Folhas Sul D-33/S e E-32/Z, 1:250 000. UTE PLANAGEO (IGME, LNEG, IIA), IGEO, Luanda (Angola), 199 p.

Escuder-Viruete, J., & Gumiel, J. C. (2021). Notícia explicativa da carta geológica da Andulo. Folha SUL C-33/X (metade Sul). Escala 1:250 000. UTE PLANAGEO (IGME, LNEG, IIA), IGEO, Luanda (Angola), 227 p.

Farr, H., Phillips, D., Maas, R., & de Wit, R. (2018). Petrography, Sr-isotope geochemistry and geochronology of the Nxau Nxau kimberlites, north-west Botswana. Mineralogy and Petrology, 112, 625-638.

Galán, G. (2021). Notícia explicativa da carta geológica do Quipungo. Folha Sul D-33/O. Escala 1:250 000. UTE PLANAGEO (IGME, LNEG, IIA), IGEO, Luanda (Angola), 194 p.

Issa Filho, A., Dos Santos, A. B. R. M. D., Riffel, B. F., Lapido-Loureiro, F. E. V., & McReath, I. (1991). Aspects of the geology, petrology and chemistry of some Angolan carbonatites. Journal of Geochemical Exploration, 40, 205-226.

Jelsma, H., Barnett, W., Richards, S., & Lister, G. (2009). Tectonic setting of kimberlites. Lithos, 112S, 55-165.

Jelsma H., Phillips, D., Joy, S., Costa, J., Facatino, M., Posser, A., Kumar, M., Wallace, C., Chinn, I., & Henning, A. (2013). Kimberlites from Central Angola: A Case Study of Exploration Findings. In:

Pearson et al. (eds), Proceedings of 10th International Kimberlite Conference. Springer, New Delhi, pp. 173-190.

Jelsma, H. A., deWit, M.J., Thiart, C., Dirks, P. H. G. M., Viola, G., Basson, I. J., & Anckar, E. (2004). Preferential distribution along transcontinental corridors of kimberlites and related rocks of Southern Africa. South African Journal of Geology, 107, 301-324.

Jourdan, F., Féraud, G., Bertrand, H., & Watkeys, M. K. (2007). From flood basalts to the inception of oceanization: Example from the $^{40}Ar/^{39}Ar$ high-resolution picture of the Karoo large igneous province. Geochemistry, Geophysics, Geosystems, 8(2), 20 p. https://doi.org/10.1029/2006GC001392

Lapido-Loureiro, F. E. V. (1973). Carbonatitos de Angola. Memórias e Trabalhos do Instituto de Investigações Cientificas de Angola, 11.

Lapido-Loureiro, F. E. V. (1968). Sub-volcanic carbonatite structures of Angola. XXIII International Geological Congress, Praga, pp. 147-161.

Lapido-Loureiro, F. E. V. (1995). A mega-província carbonatítica Brasil-Angola e os seus recursos minerais; geologia, petrografia, geoquímica, geologia económica. PhD Thesis, Universidade de Lisboa, 191 p.

Le Roex, A. P., & Lanyon, R. (1998). Isotope and trace element geochemistry of Cretaceous Damaraland lamprophyres and carbonatites, northwestern Namibia: evidence for plume-lithosphere interaction. Journal of Petrology, 39, 1117-1146.

Linol, B., de Wit, M. J., Barton, E., Guillocheau, F., de Wit, M. C. J., & Colin J. P. (2015). Facies analyses, chronostratigraphy and paleo-environmental reconstructions of Jurassic to Cretaceous Sequences of the Congo Basin. In: de Wit et al. (eds), Geology and Resource Potential of the Congo Basin. Regional Geology Reviews, Springer-Verlag, pp. 135-161.

Ludwig, K. R. (2003). Isoplot 3.00 A Geochronological Toolkit for Microsoft Excel. Berkeley Geochronology Center, Special Publication No. 4.

Machado, F. S. (1959). The volcanic Belt of Angola and its Carbonatites. Leopoldville Meetings, Commission for Technical Co-operation in Africa South of the Sahara, Leopolville, pp. 309-137.

Marsh, J. S., & Swart, R. (2018). The Bero Volcanic Complex: Extension of the Paraná-Etendeka Igneous Province into SW Angola. Journal of Volcanology and Geothermal Research, 355, 21-31.

Marzoli, A., Melluso, L., Morra, V., Renne, P. R., Sgrosso, I., D'Antonio, M., Duarte-Morais, L., Morais, E. A. A., & Ricci, G. (1999). Geochronology and petrology of Cretaceous basaltic magmatism in the Kwanza basin (western Angola) and relationships with the Parana-Etendeka continental basalt province. Journal of Geodynamics, 28, 341-356.

Melgarejo, J. C., Costanzo, A., Bambi, A. C., Gonçalves, A. O., & Neto, A. B. (2012). Subsolidus processes as a key factor on the distribution of Nb species in plutonic carbonatites: The Tchivira case, Angola. Lithos, 152, 187-201.

Mendes, F. (1968). Mésures Géochronologiques en Angola. PhD Thesis, Clermont-Ferrand, 21 p.

Merino-Martínez, E. (2022). Notícia explicativa da carta geológica da Lola. Folha 316. Escala 1:100 000. UTE PLANAGEO (IGME, LNEG, IIA), IGEO, Luanda (Angola), 184 p.

Merino-Martínez, E., Chinchilla, D., & Chamizo-Borreguero, M. (2021). Notícia explicativa da carta geológica do Ucu Seles (metade Sul). Folha Sul C-33/U. Escala 1:250 000. UTE PLANAGEO (IGME, LNEG, IIA), IGEO, Luanda (Angola), 186 p.

Merino-Martínez, E., & Goicoechea, P. (2021). Notícia explicativa da carta geológica do Lubango. Folha Sul D-33/N. Escala 1:250 000. UTE PLANAGEO (IGME, LNEG, IIA), IGEO, Luanda (Angola), 242 p.

Milner, S. C., le Roex, A. P., & O'Connor, G. M. (1995). Ages of Mesozoic igneous rocks in northwestern Namibia, and their relationship to continental breakup. Journal Geological Society London, 152, 97-104.

Morbidelli, L., Gomes, C. B., Beccaluva, L., Brotzu, P., Conte, A., Ruberti, E., & Traversa, G. (1995). Mineralogical, petrological and geochemical aspects of alkaline and alkaline-carbonatite associations from Brazil. Earth Science Reviews, 39, 135-168.

Moore, A., Blenkinsop, T., & Cotterill, F. W. (2008). Controls on post-Gondwana alkaline volcanism in Southern Africa. Earth and Planetary Science Letters, 268, 151-164. https://doi.org/10.1016/j.epsl.2008.01.007

Oliveira, A. L., Schmitz, M. D., Wall, C. J., Crowley, J. L., Macêdo Filho, A. A., & Hollanda, M. H. B. M. (2023). New U–Pb geochronology for the Central Atlantic Magmatic Province, critical reevaluation of high-precision ages and their impact on the end-Triassic extinction event. Science Reports, 13, 5485. https://doi.org/10.1038/s41598-023-32534-3.

Peate, D. W., Hawkesworth, C. J., & Mantovani, M. S. M. (1992). Chemical stratigraphy of the Paraná lavas (South America): classification of magma types and their spatial distribution. Bulletin of Volcanology, 55, 119-139.

Renne, P. R., Ernesto, M., Pacca, I. G., Coe, R. S., Glen, J. M., Prévot, M., & Perrin, M. (1992). The age of Paraná flood volcanism, rifting of Gondwanaland, and the Jurassic–Cretaceous boundary. Science, 258, 975-979.

Renne, P. R., Glen, J. M., Milner, S. C., & Duncan, A. R. (1996). Age of Etendeka flood volcanism and associated intrusions in southwestern Africa. Geology, 24, 659-662.

Renne, P. R., Swisher, C. C., Deino, A. L., Karner, D. B., Owens, T. L., & DePaolo, D. J. (1998). Intercalibration of standards, absolute ages and uncertainties in $^{40}Ar/^{39}Ar$ dating. Chemical Geology, 145 (1-2), 117-152.

Riccomini, C., Velázquez, V. F., & Gomes, C. B. (2005). Tectonic controls of the Mesozoic and Cenozoic alkaline magmatism in central-southeastern brazilian platform. In: Comin-Chiaramonti and Gomes (eds.), Mesozoic to Cenozoic Alkaline Magmatism in the Brazilian Platform. Edusp Fapesp, São Paulo, Brazil, pp. 31-55.

Robles Cruz, S. E. (2013). Kimberlites associated with the Lucapa structure, Angola. PhD Thesis, Universitat de Barcelona, 112 p.

Robles-Cruz, S. E., Escayola, E., Jackson, S., Galí, S., Pervov, V., Watangua, M., Gonçalves, A., & Melgarejo, J. C. (2012). U–Pb SHRIMP geochronology of zircon from the Catoca kimberlite, Angola: Implications for diamond exploration. Chemical Geology, 310-311, 137-147.

Schärer, U., Corfu, F., & Demaiffe, D. (1997). U–Pb and Lu–Hf isotopes in baddeleyite and zircon megacrysts from the Mbuji-Mayi kimberlite: constraints on the subcontinental mantle. Chemical Geology, 143, 1-16.

Silva, A. T. F., Torquato, J. R., & Kawashita, K. (1973). Alguns dados geocronológicos pelo método K/Ar da região de Vila Paiva Couceiro, Quilengues e Chicomba (Angola). Serviço de Geologia e Minas de Angola, 24, 29-46.

Svensen, H. H., Torsvik, T. H., Callegaro, S., Augland, L., Heimdal, T. H., Jerram, D. A., Planke, S., & Pereira, E. (2017). Gondwana Large Igneous Provinces: plate reconstructions, volcanic basins and sill volumes. In: Sensarma and Strorey (eds), Large Igneous Provinces from Gondwana and Adjacent Regions. Geological Society, Special Publications, 463, pp. 17-40.

Torquato, J. R. (1977). Geotectonic Outline of Angola. Cahiers de l'Office de la Recherché Scientífique et Technique Outre-Mer (O.R.S.T.O.M.), Série Geólogie, 9 (1/2), 15-34.

Torquato, J. R., & Amaral, G. (1973). Idade K/Ar em rochas de Catanda e Vila de Almoster. Instituto de Investigação Científica de Angola, Boletim, 10 (1), 89-95.

Torsvik, T. H., Rousse, S., Labails, S., & Smethurst, M. A. (2009). A new scheme for the opening of the South Atlantic Ocean and the dissection of an Aptian salt basin. Geophysics Journal International, 177, 1315-1333.

Vale, F. S., Graça da Cruz, A., Simões, M., & Pereira, E. (1972). Carta Geológica de Angola, à escala 1:100.000. Folha 316 (Dinde-Lola). Direcção Provincial dos Serviços de Geologia e Minas, Angola.

Woolley, A. R. (2001). Alkaline Rocks and Carbonatites of the World. Part 3: Africa. The Geological Society of London, 372 p. ISBN: 1–86239–083–5